

Demonstration of the course of the posterior intercostal artery on CT angiography: relevance to interventional radiology procedures in the chest

Catherine Dewhurst, Siobhan O'Neill, Kevin O'Regan, Michael Maher

PURPOSE

To document the course of the posterior intercostal artery (PIA) within the intercostal space (IS) *in vivo* using computed tomography angiography (CTA).

MATERIALS AND METHODS

A review of 428 IS from CTA of the chest was performed. Using multiplanar reconstruction (MPR) algorithms, the course of the PIA within the IS and the maximum distance of the PIA from the undersurface of the rib were determined in the 4th to 8th IS at three clinically relevant points: the posterior paravertebral area (PPV), angle of the rib (AR), and 25 mm lateral to the angle of the rib (LAR). Tortuosity of the vessels was graded from coronal three-dimensional images.

RESULTS

The mean maximum distances of the PIA within the IS from the undersurface of the rib were as follows: PPV, 7.2 ± 0.512 mm ($P = 0.0027$); AR, 5.5 ± 0.535 mm ($P = 0.0487$); and LAR, 2.3 ± 0.366 mm ($P = 0.0052$). At the PPV, the PIA lies halfway between the two ribs within the IS and lies one third of the way from the undersurface of the rib at the AR and comes to lie within the subcostal groove toward the mid-axillary line. The tortuosity of the vessel was highly variable and was independent of both age and gender.

CONCLUSION

Considerable variability in vessel position was noted within the IS, with the PIA lying furthest from the undersurface of the rib in the PPV. To avoid injury, our data support the dictum "choose a site above the rib below," and additional caution should be taken to avoid the posterior paravertebral area.

Key words: • computed tomography • interventional radiology • hemothorax

The anatomical course of the posterior intercostal artery (PIA) is of particular importance to interventional radiologists who perform procedures that require traversal of the posterior intercostal space for both diagnostic and therapeutic purposes. Percutaneous transthoracic interventions, such as thoracentesis and lung biopsy, are well-established procedures and are being performed with increasing frequency in clinical practice (1–9). The reported rates of PIA laceration vary within the literature, but the overall incidence rate is less than 1%. However, this figure may even be an overestimation of the actual incidence as it is a vanishing complication now rarely encountered in everyday practice (10–13). Inadvertent laceration of the PIA during percutaneous thoracic intervention can result in significant hemothorax and is associated with high rates of morbidity and mortality; thus, knowledge regarding the course of the PIA is of great importance.

Despite the increasing frequency of percutaneous transthoracic intervention and the availability of excellent cross-sectional imaging techniques, the anatomical course of the PIA within the intercostal space (IS) *in vivo* has not been widely described in the literature, and only one other recent study has discussed its importance in interventional radiology (14). Computed tomography angiography (CTA) is a valuable tool for depicting vascular anatomy in a wide variety of anatomical regions. With excellent spatial resolution and rapid acquisition, CTA is used clinically to evaluate vessels as small as 1 mm in diameter and has been applied to imaging of the coronary, renal, cerebral, and pulmonary systems (15).

Traditional anatomical teaching suggests that the PIA lies within the costal groove, which is located along the inferior portion of the rib. However, in anatomical dissections using human cadavers, considerable variation has been seen in the positions of the neurovascular bundles, which may be located at a variable distance below the costal groove. The diameter of the IS in anatomical specimens has been shown to decrease as it courses anteriorly (16–19).

The purpose of this study was to document the course and tortuosity of the PIA within the IS *in vivo* using CTA.

Materials and methods

This retrospective study was initiated following Institutional Review Board (IRB) approval. Seventy-five consecutive patients who underwent CTA or CT pulmonary angiography (CTPA) for a range of clinical indications over a six-month period from January to July 2009 were included in this study. Exclusion criteria consisted of chest wall deformity or a history of previous thoracic surgery in 16 patients, pregnancy in two patients, and sub-optimal evaluation of the contrast bolus precluding visualization of the PIA in seven patients. Therefore,

From the Department of Radiology (C.D. ✉ cathydewhurst@gmail.com), Cork University Hospital, Cork, Ireland.

Received 23 March 2011; revision requested 16 May 2011; revision received 30 May 2011; accepted 9 June 2011.

Published online 28 November 2011
DOI 10.4261/1305-3825.DIR.4366-11.1

the study group consisted of 50 patients (male:female, 23:27) with a mean age of 63.7±18.77 years (range, 21–96 years). Thirty-two patients underwent CPTA and 18 patients underwent CTA. Data were collected by a radiology resident (C.D.) and two board-certified radiologists (K.O.R. and M.M.), all of whom reported and logged relevant data in consensus.

The 4th to the 8th IS were used for measurements as they are the most common positions for chest interventional radiology procedures; they were visualized and present in all 50 patients and are included in the scan plane for both CTPA and CTA. A total of 428 out of a possible 500 PIA in the IS were evaluated; some of the arteries were not clearly visualized in the lower spaces, and this was secondary to an either poor contrast bolus and opacification of the vessel or not being able to fully evaluate the vessel entirely along its length.

CTA was performed on our four-row helical scanner (Aquilion MDCT, Toshiba America Medical Systems, Tustin, California, USA) using a standard contrast-enhanced protocol for CTA or CTPA. CT images were obtained during patient breath-holding using the following parameters: 120 kVp, 200–400 mA (depending on patient size), with a section thickness of 2.5 mm and an axial reconstruction interval of 2.5×2.5 mm for CTA, and a slice thickness of 5 mm and axial reconstruction interval of 5×5 mm for CTPA. A 120-mL dose of nonionic intravenous contrast material (Iohexol 300, Omnipaque, GE Healthcare, Milwaukee, Wisconsin, USA) was administered with a power injector at a rate of 4.0 mL/s (or slower if mandated due to suboptimal venous access). All images were reviewed and reconstructed on a Vitrea Workstation (Vital Images Inc., Minnetonka, Minnesota, USA).

Multiplanar reconstructions were performed on a Vitrea Workstation (Vital Images Inc.). Images were reconstructed in the coronal plane using volume-rendered maximum intensity projections (MIP) with a slice thickness of 7.00 mm and a window settings of 1200 (width) × 300 (center). Readers were aware that patients were being evaluated for PIA measurements, but they were blinded to all other clinical, pathological, and imaging findings. Prior to

image interpretation, the readers met and agreed on the CT features to be used to measure the PIA and designed a data collection form.

Image analysis

The distance of PIA from the undersurface of the upper rib was measured at three clinically relevant points: the posterior paravertebral level (PPV), angle of the rib (AR), and 25 mm lateral to the angle of the rib (LAR). The LAR point was chosen as this most accurately defined the mid-axillary level. The maximum height of the IS was also calculated at the same positions. The results were recorded on both sides from the 4th to the 8th IS.

Qualitative analysis of vessel tortuosity was performed using the grading system described below (Table 1). Tortuosity was described subjectively on a scale of 0 to 3 (8). A reading of 0 described a straight vessel, running parallel and close to the undersurface of the rib, whereas a reading of three closely resembled a “sine wave pattern.” Both interpreters reached a consensus regarding the grading of the PIA within the IS. Tortuosity was defined as the deviation of the PIA from the undersurface of the rib according to the scale devised.

Statistical analysis

The Pearson’s correlation coefficient was calculated to measure the strength of the correlation of the distance of the PIA from the undersurface of the rib in the IS. This analysis was performed using SAS software (version 9.1; SAS Institute, Cary, North Carolina, USA). In all analyses, $P < 0.05$ was taken to indicate statistical significance.

Results

The PIA was clearly visualized in 428 out of a possible of 500 IS; therefore, these vessels and their corresponding spaces were evaluated. There were no significant differences between the visualization of the PIA in the IS between CTA and CTPA: 87% were clearly visualized with CTPA (279 of a possible 320 IS) and 83% were clearly visualized with CTA (149 of a possible 180 IS) ($P = 0.65$).

Intercostal space: The mean vertical width of the IS, as measured from the inferior border of the overlying rib to the superior border of the underlying rib, was found to increase in the cranio-caudal direction and decrease when moving laterally within the spaces measured in concordance with the results of previous anatomical dissections ($P = 0.0947$) (Table 2, Fig.).

Posterior paravertebral space: The mean maximum distance of the PIA below the undersurface of the rib within the IS was 7.2±0.512 mm (range, 1.9–17.5 mm). The wide range was due to an increase in the mean deviation in the caudal direction ($P = 0.0027$) and was also a consequence of inconsistent anatomical location (Table 3, Fig.).

Angle of the rib: The mean maximum distance of the PIA below the undersurface of the rib within the IS was 5.5±0.535 mm (range, 0–17.8 mm). The location of the PIA within the intercostal space relative to the rib above showed a wide degree of variation, with an increase in deviation seen in the lower intercostal spaces ($P = 0.0487$) (Table 3, Fig.).

Lateral to the angle of the rib: Little deviation of the PIA from the undersurface of the rib was observed lateral

Table 1. Tortuosity grading system for the posterior intercostal artery within the intercostal space (n=248)

Tortuosity	Description	Grade	Intercostal space n (%)
	Linear	0	32 (7.4)
	Slight curve	1	152 (35.5)
	Wavy	2	169 (39.4)
	Sinusoidal	3	75 (17.5)

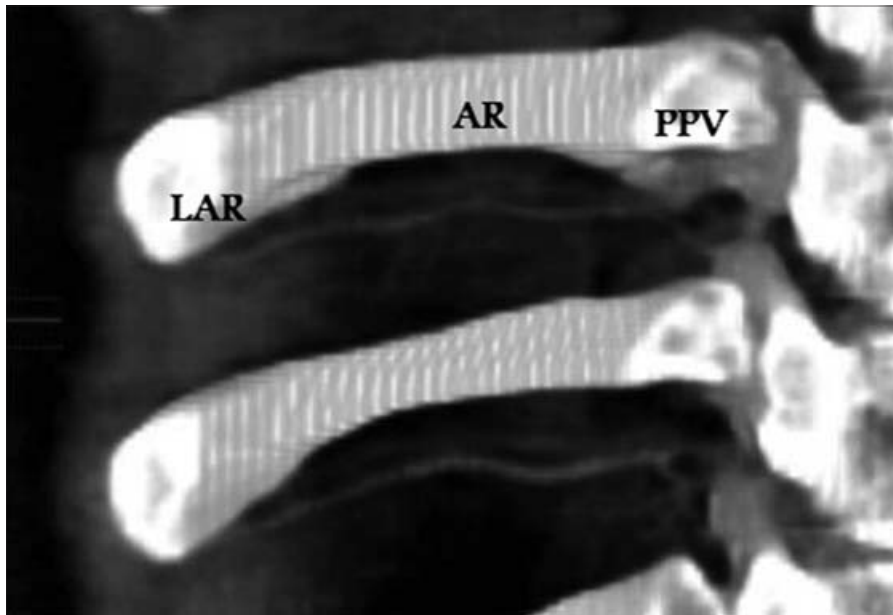


Figure. Multiplanar reconstruction coronal oblique contrast-enhanced CT of the chest demonstrating the tortuosity of the posterior intercostal artery (PIA) in the the intercostal space (IS) and its maximum deviation below the undersurface of the rib calculated at the posterior paravertebral (PPV) level, at the angle of the rib (AR), and lateral to the angle of the rib (LAR). It also demonstrates the variability in tortuosity of the PIA as it lies within IS and thus the precise location of the PIA is difficult to predict especially at the PPV level and at the AR.

to the angle of the rib, the area that approximates the mid-axillary line (mean deviation of 2.3 ± 0.366 mm; range, 0–5.2 mm). There was also less variation in the observed distance, indicating a more consistent location of the PIA when compared to the PPV or the AR ($P = 0.0052$) (Table 3, Fig.).

Tortuosity: Tortuosity was defined subjectively on a scale of 0–3 (8). Over 75% of the PIA had either grade 1 or 2 tortuosity. Our results showed that tortuosity is highly variable, and statistical analysis showed it to be independent of both age ($P = 0.79$) and gender ($P = 0.65$).

Discussion

A posterior intercostal approach is frequently used during interventional radiology procedures to gain access to the thoracic cavity. The anatomical course of the PIA is of clinical importance in this context since inadvertent injury during percutaneous transthoracic intervention can have serious consequences, including hematoma or hemothorax. While conventional anatomical teaching has proposed that the neurovascular bundle, containing the PIA, lies within the subcostal groove in the superior portion of the IS, observations from clinical practice suggest significant inter-individual variability and aberrancy.

Cadaveric studies have shown that the more cephalad PIAs originate about two segmental levels below their feeding levels, whereas the segmental arteries originate just below the corresponding vertebra for the lower thoracic and upper lumbar vertebrae. Each segmental artery then runs upward to reach the corresponding IS, thus giving a more apparent ascending course in the upper thoracic region. Dissection studies have also demonstrated considerable variation in the position of the neurovascular bundle, which may be located at varying distances below the costal groove within the IS (16, 19, 20).

CTA demonstrates considerable variability in the course of the PIA. Medially, in the posterior paravertebral region, the PIA lies approximately in the middle of the IS, equidistant from the upper and lower ribs. Moving laterally, the PIA deviates superiorly and lays approximately one third of the way from the superior rib at the AR, and comes to lie in the subcostal groove 25 mm LAR. It appears that the

Table 2. Mean width of the intercostal space in the craniocaudal direction

Intercostal space number	Width (mm) (mean±standard deviation)
4	12.90±2.64
5	15.40±2.96
6	17.20±3.64
7	18.59±4.85
8	20.57±4.35

Table 3. Pearson correlation coefficient was used to determine the relationship between the deviation of the posterior intercostal artery from the undersurface of the rib in the intercostal space, at the posterior paravertebral level, angle of rib, and lateral to angle of the rib

Level	PIA ^a (n=428)	IS ^a (n=428)	P
PPV	7.19±0.51	14.6±2.8	0.0027
AR	5.51±0.53	153±2.4	0.0487
LAR	2.26±0.36	12.3±2.1	0.0052

PIA, posterior intercostal artery; IS, intercostal space; PPV, posterior paravertebral level; AR, angle of rib; LAR, lateral to angle of the rib.

^ameasured in mm, mean±standard deviation.

rib offers more protection to the PIA laterally than medially, thus favoring the mid-axillary line approach for transthoracic interventions and avoidance of the paravertebral space (14).

In a caudal direction, from the 4th to the 8th intercostal space, there is a significant increase in the mean width of the IS allowing the PIA to dip more significantly into the IS at the lower levels. Conversely, there is a significant progressive decrease in the mean width of the IS when traveling laterally, with a maximal width at PPV. This results in a decrease in the lateral vulnerability of the PIA as it dips less into the IS.

Vessel tortuosity grades indicated that this was also unpredictable, independent of both age and gender, and could be either straight or extremely complex in shape and location. This differs from the results of a previous study by Choi et al. (15) who examined only 160 IS, but concluded that there was increased tortuosity of the vessel with increasing age; this was not observed in the present study ($P = 0.79$) and there were no differences between the right and left sides.

Thus, while cadaveric specimens have shown variability of the PIA within the IS, the present study defined its position *in vivo* using CTA. While this study was limited by the small number of patients, our data support the conclusion that the PIA is variable in position and tortuosity, particularly at the PPV junction. In addition, our study was limited to a four-slice MDCT, and with the advent of 64-slice imaging, image quality and vascular anatomy can now be much better defined.

In conclusion, our data suggest the presence of high variability and tortuosity of the PIA, particularly at the PPV

and AR. While the principle of “choosing a site above the rib below” is endorsed in the context of percutaneous transthoracic intervention, we would advocate the addition of increased caution to avoid the posterior paravertebral space to this dictum, as there is a potentially increased risk of inadvertent vessel injury in this area.

Conflict of interest disclosure

The authors declared no conflicts of interest.

References

1. Kwan S, Bhargavan M, Kerlan R, et al. Effect of advanced imaging technology on how biopsies are done and who does them. *Radiology* 2010; 256:751–758.
2. Gupta S, Seaberg K, Wallace M, et al. Imaging guided percutaneous biopsy of mediastinal lesions: different approaches and anatomic considerations. *Radiographics* 2005; 25:763–788.
3. Paulson E, Sheafor D, Enterline D, et al. CT fluoroscopy-guided interventional procedures: techniques and radiation dose to radiologists. *Radiology* 2001; 220:161–167.
4. Wallace M, Krishnamurthy S, Broemeling L, et al. CT-guided percutaneous fine-needle aspiration biopsy of small (≤ 1 cm) pulmonary lesions. *Radiology* 2002; 225:823–828.
5. Tomlinson MA, Treasure T. Insertion of a chest drain: how to do it. *Br J Hosp Med* 1997; 58:248–252.
6. Laws D, Neville E, Duffy J. BTS guidelines for the insertion of a chest drain. *Thorax* 2003; 58:53–59.
7. Al-Tarshihi MI, Khamash FA, Al Ibrahim AEO. Thoracoscopy tube complications and pitfalls: an experience at tertiary level military hospital. *RMJ* 2008; 33:141–144.
8. Ko JP, Shepard JO, Drucker EA, et al. Factors influencing pneumothorax rate at lung biopsy: are dwell time and angle of pleural puncture contributing factors? *Radiology* 2001; 218:491–496.
9. Utz JP, Ryu JH, Douglas WW, et al. High short-term mortality following lung biopsy for usual interstitial pneumonia. *Eur Respir J* 2001; 17:175–179.

10. Yamauchi H, Amemiya R, Shida D, et al. A case of spontaneous hemopneumothorax associated with uncontrolled massive bleeding after insertion thoracic drain. *Jap J Thorac Surg* 1999; 52:965–968.
11. Muthuswamy P, Samuel J, Mixcock B, et al. Recurrent massive bleeding from an intercostal artery aneurysm through an empyema chest tube. *Chest* 1993; 104:637–639.
12. Carney M, Ravin CE. Intercostal artery laceration during thoracocentesis: increased risk in elderly patients. *Chest* 1979; 75:520–522.
13. Seneff MG. Complications associated with thoracocentesis. *Chest* 1986; 90:97–100.
14. Yacovone M, Kartan R, Bautista M. Intercostal artery laceration following thoracocentesis. *Respir Care* 2010; 55:1495–1498.
15. Choi S, Trieu J, Ridley L. Radiological review of intercostal artery: anatomical considerations when performing procedures via intercostal space. *J Med Imaging Radiat Oncol* 2010; 54:302–306.
16. Oguz B, Haliloglu M, Karcaaltincaba M. Paediatric multidetector CT angiography: spectrum of congenital thoracic vascular anomalies. *Br J Radiol* 2007; 80:376–383.
17. Wraight WM, Tweedie DJ, Parkin IG. Neurovascular anatomy and variation in the fourth, fifth and sixth intercostal spaces in the midclavicular line: a cadaveric study in respect of chest drain insertion. *Clin Anat* 2005; 18:346–349.
18. Da Rocha RP, Vengjer A, Blanco A, de Carvalho PT, Mongon ML, Fernandes GJ. Size of the collateral intercostal artery in adults: anatomical considerations in relation to thoracocentesis and thoracoscopy. *Surg Radiol Anat* 2002; 24:23–26.
19. Muzrakchi AA, Szmigielski W, Omar AJ, et al. Is the 10th and 11th intercostal space a safe approach for percutaneous nephrostomy and nephrolithotomy? *Cardiovasc Intervent Radiol* 2004; 27:503–506.
20. Davies DV. *Gray's anatomy*. 34th edition. London: Longmans, Green and Co. 1967.